Published in final edited form as:

Nat Chem Biol. 2017 October ; 13(10): 1109–1114. doi:10.1038/nchembio.2459.

Metals induce transient folding and activation of the Twister ribozyme

Subrata Panja[1,*], **Boyang Hua**[2], **Diego Zegarra**[1], **Taekjip Ha**[1,2,3], and **Sarah A. Woodson**[1]

[1]T. C. Jenkins Department of Biophysics, Johns Hopkins University, 3400 N. Charles St., Baltimore, MD 21218 USA

[2]Department of Biophysics and Biophysical Chemistry, Johns Hopkins School of Medicine, 725 Wolfe St., Baltimore, MD 21205 USA

[3]Howard Hughes Medical Institute, Baltimore, MD 21205 USA

Abstract

Twister is a small ribozyme present in almost all kingdoms of life that rapidly self-cleaves in variety of divalent metal ions. We used activity assays, bulk FRET and single-molecule FRET (smFRET) to understand how different metal ions promote folding and self-cleavage of the *Oryza sativa* Twister ribozyme. Although most ribozymes require additional Mg^{2+} for catalysis, Twister inverts this expectation, requiring 20–30 times less Mg^{2+} to self-cleave than to fold. Transition metals such as Co^{2+}, Ni^{2+} and Zn^{2+} activate Twister more efficiently than Mg^{2+} ions. Although Twister is fully active in ≤ 0.5 mM $MgCl_2$, smFRET experiments showed that the ribozyme visits the folded state infrequently under these conditions. Comparison of folding and self-cleavage rates indicates that most folding events lead to catalysis, which correlates with metal bond strength. Thus, the robust activity of Twister reports on transient metal ion binding under physiological conditions.

Keywords

Twister ribozyme; self cleaving RNA; metal ions; RNA folding; single-molecule FRET

[*]Corresponding author: spanja2@jhu.edu; tel. 410-516-7348; FAX 410-516-4668.

Author contributions

S.P., T.H. and S.W. designed the experiments; S.P. and B.H. performed the single-molecule experiments and analyzed the data; S.P. and D.Z. performed activity assays; S.P. performed other experiments; S.P, T.H. and S.W. wrote the manuscript; and all of the authors interpreted the data and reviewed the text and figures.

Competing financial interests

The authors declare no competing financial interests.

Data Availability

All data including single molecule trajectories are available from the authors upon request to S. Panja (corresponding author) or to swoodson@jhu.edu.

Code Availability

All custom software and codes mentioned above are available upon request to tjha@jhu.edu.

Catalytic RNA is found in almost all kingdoms of life and thought to be a relic of an RNA-based world[1]. Recent discoveries of new classes of small self-cleaving ribozymes in a wide number of natural genomes[2,3] raise questions about the range of physiological conditions that support RNA catalysis. Mg^{2+} ions are usually thought to stabilize the folded structures that are necessary for the biological functions of ribozymes and other noncoding RNAs. Nevertheless, the findings that certain riboswitches sense Ni^{2+} or Co^{2+} (ref. 4) and Mn^{2+} (ref. 5) demonstrate that transition metal ions can also support the biological functions of RNA[6]. Because the RNA tertiary structure provides a frame for catalysis and ligand recognition, stably folded RNAs are generally expected to be more active than unstable RNAs. Indeed, many ribozymes require more Mg^{2+} for catalytic activity than for folding.

Twister self-cleaving ribozymes were recently discovered through a bioinformatics search, and are widespread among microbial, plant and animal genomes[2]. The Twister ribozyme from *Oryza sativa* (*Osa*) contains three conserved paired regions, P1, P2 and P4, separated by flexible loops[2,7] (Fig. 1a). In some Twister ribozymes, an additional P3 helix is inserted between helix P2 and P4. Phylogenetic analyses[2] and X-ray crystallography[7] have shown that the L2–L4 and L4–L1 loops form two pseudoknots that fold Twister into a compact tertiary structure (Fig. 1b). The “twisted” tertiary structure forms an active site pocket that catalyzes cleavage of the phosphodiester bond between U6 and A7 (Fig. 1a,b).

Although metal ions are not thought to be required for Twister catalysis, metal ions are needed to stabilize the overall fold[2] and organize the active site[8,9]. Initial studies showed that the non-bridging phosphate oxygens and the 5′ oxyanion leaving group do not form inner-sphere contacts with divalent metal ions[2], and the divalent metal ions do not contribute directly to catalysis. Instead, conserved nucleobases within the active site stabilize the transition state for cleavage of the scissile phosphodiester bond[9]. These include G33 and A1, which are proposed to act as a general base and general acid, respectively[10,11]. Nevertheless, metal ions are present in the active site and may contribute to catalysis, directly or indirectly[12]. In crystal structures of an environmental (*env*22) Twister ribozyme, electron density was assigned to a hydrated Mg^{2+} near the scissile phosphodiester[8,2]. Thus, by analogy with other small ribozymes, it was expected that full stabilization of the Twister active site would require high Mg^{2+} concentrations, in excess of what is needed to fold the RNA.

Here, we report that the small Twister ribozyme requires less Mg^{2+} to self-cleave than to fold, in contrast to our expectations. We also found that Twister becomes active in lower quantities of transition metals than of Mg^{2+} ions, raising the possibility that Twister responds to transition metals in the cell. Thus, unlike other ribozymes which require a stable tertiary structure for maximum activity, our results show that transient folding in micromolar Mg^{2+} or transition metal ions is sufficient for maximal self-cleavage by the *Osa* Twister ribozyme.

RESULTS

Self-cleaving activity of Twister ribozyme in $MgCl_2$

To understand how self-cleaving activity depends on the presence of divalent metal ions, we measured the rate of self-cleavage in different $MgCl_2$ concentrations. For self-cleavage experiments, we initially used a bimolecular form of *Osa* Twister ribozyme that has an extended P3 helix and forms a stable complex between the "ribozyme" and "substrate" RNAs (Fig. 1a)[2,7]. We used a ribozyme with a stable 5 bp P1 helix, because we found that this increased the reactivity of our ribozyme in comparison to a variant with a 3 bp P1 (Supplementary Results, Supplementary Fig. 1). This observation is supported by the finding that for proper folding of the central pseudoknot (Fig. 1a), the P1 stem must form correctly[13], contrary to reports that P1 is not required for self-cleavage of the *env22* Twister[14].

To start the reaction, $MgCl_2$ was added to the pre-assembled ribozyme–substrate complex at 20 ˚C, and the cleaved product was detected by denaturing PAGE (Fig. 1c). At very low $MgCl_2$ concentrations (50 μM), a single exponential increase in cleaved product corresponded to an observed rate constant k_{obs} = 0.24 min^{-1} at pH 7.5 (Fig. 1d). At 0.5 mM $MgCl_2$ and above, the initial rate of self-cleavage increased to 8.4 min^{-1}. This initial phase was followed by a slower kinetic phase (k_{obs} = 0.6 min^{-1}) that may reflect an additional conformational rearrangement of the active site pocket predicted by MD simulations and crystallographic structures[8,15]. These rates of self-cleavage were roughly comparable to those of an environmental Twister sequence at pH 7.5 and 50 μM $MgCl_2$ (k_{obs} ~0.1 min^{-1})[2] and *env22* Twister ribozyme at 10 mM $MgCl_2$ (k_{obs} = 2.4 min^{-1})[8].

To determine the sensitivity of Twister activity to $MgCl_2$ concentration, we measured the extent of self-cleavage of the bimolecular Twister RNA after 1 min at different $MgCl_2$ concentrations (Fig. 1e). This 1-min interval corresponds to the end of the fast phase of self-cleavage, which is the phase that is most sensitive to $MgCl_2$ concentration. The fraction of RNA cleaved at different $MgCl_2$ concentrations is well-fit by a two-state cooperative folding equilibrium with a midpoint of 135 (±12) μM $MgCl_2$ that saturates around 2 mM $MgCl_2$ (Fig. 1f). Thus, Twister ribozyme is fully active in physiological Mg^{2+} levels, which are reported to be 1–5 mM in bacteria[16,17] and 5 mM in plant phloem[18].

We also determined the $MgCl_2$ requirement for self-cleavage of the unimolecular form of the *Osa* Twister ribozyme, which has a short P3 stem (Fig. 1a). Although 40% of the RNA was cleaved during sample preparation (Fig. 1g), we were able to measure the Mg^{2+}-dependence of self-cleavage for the remaining precursor RNA. The unimolecular form of the Twister ribozyme was even more reactive than the bimolecular form, with a midpoint of 65 (±6) μM $MgCl_2$ (Fig. 1h).

Folding of Twister monitored by RNase footprinting

To test whether the level of Twister self-cleavage correlates with the extent of folding, we compared the folding midpoints of the bimolecular and unimolecular Twister ribozymes at 20 °C using RNase footprinting. G21 and G35 are protected from cleavage by RNase T1 when the two pseudoknots become paired (Supplementary Figs. 2 and 3). Unexpectedly,

both forms of the ribozyme required higher Mg^{2+} concentrations to fold than to self-cleave (Fig. 1f,h). The midpoint for protection of G21 in the bimolecular Twister with increasing $MgCl_2$ concentration was 2.5 mM $MgCl_2$ (Fig. 1f), 20 times higher than the midpoint for catalysis (0.135 mM $MgCl_2$). For the unimolecular ribozyme, the midpoint for protection of G21 was ~1.8 mM (Fig. 1h), 27 times higher than the midpoint for catalysis (0.065 mM $MgCl_2$).

RNA folding by ensemble FRET

To measure folding thermodynamics and kinetics more precisely, we labeled the minimal unimolecular form of *Osa* Twister ribozyme with Cy3 and Cy5 fluorophores, such that folding of the two pseudoknots increases the efficiency of fluorescence resonance energy transfer (FRET) from Cy3 to Cy5 (Fig. 2a). Cy3 was inserted before U15 at the top of helix P4 (Online Methods). The 3′ end of the ribozyme was extended with DNA, and annealed to a complementary Cy5-labeled DNA oligomer (Fig. 2a). The scissile uridine (U-1) was replaced with 2′ deoxyuridine to prevent self-cleavage. The relative extent of folding was calculated from the increase in the ensemble FRET efficiency with $MgCl_2$ concentration, and fit to a cooperative two-state equilibrium model (Fig. 2b). The midpoint for folding was 10 mM $MgCl_2$ at 30 ˚C (Fig. 2b) and 13 mM $MgCl_2$ at 20 ˚C (Supplementary Fig. 4), five times higher than the midpoint obtained from RNase footprinting (1.8 mM $MgCl_2$). The increase in FRET depended on proper folding of the ribozyme, because it was abolished by mutations that destabilize either pseudoknot (Fig. 2b).

We confirmed that the labeled unimolecular form of the ribozyme self-cleaves, although the reaction is slower and much less efficient than self-cleavage of the unlabeled unimolecular ribozyme (Supplementary Fig. 5). This is likely owing to destabilization of delicate interactions within the L4 loop, because the fluorophore attachment affects cleavage more than global folding. Consistent with this view, we found that the folding midpoints of dye-labeled cleavable (rU-1) and uncleavable (dU-1) bimolecular ribozymes were similar to each other (2.1 and 2.8 mM respectively; Supplementary Fig. 6) and similar to the folding midpoint of the unlabeled RNA (2.5 mM; Supplementary Fig. 3 and Table 2). This suggests that the longer P3 helix of the bimolecular ribozyme compensates for the destabilizing effect of the fluorophores on L4. We concluded that our FRET assay can be used to measure tertiary folding (but not activity) of the Twister ribozyme, after accounting for a 5-fold shift in the Mg^{2+}-dependence of the folding transition.

RNA dynamics by single-molecule FRET

The observation that the Mg^{2+} midpoints for folding were higher than those for activity conflicts with the usual assumption that RNA must stably fold into its correct tertiary conformation to attain its maximum catalytic activity. To understand the folding dynamics of Twister ribozyme and to determine whether it transiently adopts its tertiary structure in micromolar Mg^{2+}, we used total internal reflection fluorescence (TIRF) microscopy to follow the folding of single RNAs through smFRET[19]. For smFRET studies, we used the same dye-labeled Twister ribozyme that we used for ensemble FRET, except that the RNA was immobilized on a quartz slide via a biotinylated DNA oligomer. The FRET efficiency

(E_{FRET}) was calculated from the Cy3 and Cy5 intensities after background subtraction and leakage correction[20].

As the $MgCl_2$ concentration in the smFRET experiment was increased, Twister ribozymes spent more time in the folded state, on average, as expected (Fig. 2c). In 0.5 mM $MgCl_2$, the ribozyme was mostly in a low FRET (E_{FRET} ~ 0.2) state that corresponds to the unfolded conformation (Fig. 2c, top). Occasionally, the ribozyme sampled the high FRET (E_{FRET} ~ 0.8) state corresponding to the folded conformation, remaining there for 1–2 seconds before returning to the unfolded state. With increasing $MgCl_2$ concentration, Twister sampled the high FRET state more frequently and for longer periods, approaching an equilibrium of equal probability in low and high FRET states at 15 mM $MgCl_2$. Surprisingly, even at 100 mM $MgCl_2$, which is many times higher than physiological concentrations, the ribozyme continued to sample the low FRET state (Fig. 2c, bottom), indicating that the minimal structure of the *Osa* Twister ribozyme is highly dynamic.

Histograms of E_{FRET} values were constructed from trajectories for > 200 molecules for each condition, revealing well-separated peaks in the distribution at high and low FRET efficiencies (Fig. 2d). We calculated the absolute fraction of folded ribozyme by dividing the area of the high FRET population by the total area of the histograms. The Mg^{2+} midpoint of folding from smFRET experiments was 15 mM, very similar to that obtained from ensemble FRET measurements (Fig. 2b).

Since tertiary interactions within the L4 loop are important for the stability of the folded ribozyme, we also carried out smFRET experiments with a cleavable (rU-1) unimolecular ribozyme and the non-cleavable bimolecular (dU-1) ribozyme (Supplementary Fig. 7). These RNAs exhibited comparable dynamics and distributions between folded and unfolded states, indicating that the scissile ribose and the extended P3 helix have little effect on global folding of the Twister ribozyme. All of the ribozyme forms tested occupied the folded state only transiently in 0.5 mM $MgCl_2$, although the ribozyme is fully active under comparable conditions (0.1 mM $MgCl_2$, after accounting for a fivefold shift in the folding midpoint).

It has been shown previously that crowded environments stabilize folded RNA structures[21,22,23]. When we performed smFRET experiments in the presence of molecular crowders such as PEG, the folded, high-FRET population increased from 44% in dilute solution containing 20 mM $MgCl_2$ to 65% and 70% in the presence of 10% PEG1000 and PEG8000, respectively (Supplementary Fig. 8). Yet, even in crowded solutions comparable to those in the cell, folded *Osa* Twister is marginally stable in 20 mM $MgCl_2$.

Mutations inhibit folding and self-cleaving activity

We next asked whether both pseudoknots are needed to form the high FRET conformation and whether they are necessary for self-cleavage. Twister variants containing single mismatches in pseudoknot 1 (G21A) or pseudoknot 2 (G36A) folded less than 20% even at 100 mM $MgCl_2$ (Fig. 2b). We also carried out smFRET folding experiments on the mutant Twister ribozymes. At 10 or 20 mM $MgCl_2$, we observed no transitions to the high FRET state. At 50 mM $MgCl_2$, when WT Twister is in the high FRET state most of the time, the single and double mutants only occasionally visited the high FRET state (Fig. 3a). The

folded population of the Twister mutants at 50 mM $MgCl_2$ (Fig. 3b) was comparable to that of the WT ribozyme at 2 mM $MgCl_2$ (Fig. 2d). Although the WT Twister ribozyme self-cleaved efficiently at 2 mM $MgCl_2$, we observed only 3% product for the G21A and no product for the G35A-G36A mutants at 50 mM $MgCl_2$ (Supplementary Fig. 9). We obtained similar results when transcribing the WT and Twister mutants *in vitro* (Supplementary Fig. 9d). Thus, even when the mutants transiently adopt the high FRET conformation in high Mg^{2+}, this structure is insufficient for catalysis.

Mg^{2+} ion dependence of the folding kinetics

To better understand how the dynamic tertiary structure of Twister supports rapid self-cleavage, we quantified the lifetimes of the unfolded and folded states at equilibrium by applying Hidden Markov Model analysis to selected trajectories (Fig. 4a). The probabilities of transitions from one state to the other yield rate constants for folding and unfolding, k_F and k_U. Both of these rate constants depended on Mg^{2+} concentration (Fig. 4b), with the folding rate increasing nine times between 0.5 mM and 100 mM $MgCl_2$. The slope $n_F^{\ddagger} = \partial\log(k_{fold})/\partial\log[Mg^{2+}]$ can be interpreted as an average uptake of 0.44 Mg^{2+} ions per RNA molecule upon conversion of the unfolded RNA to the folding transition state[24]. A similar analysis of unfolding rate constants suggests a loss of $n_U^{\ddagger} = 0.86$ Mg^{2+} ions during conversion of the folded state to the transition state (Supplementary Fig. 10). The calculated Hill co-efficient $n = n_U^{\ddagger} + n_F^{\ddagger} = 1.3$ exactly matched the Hill co-efficient $n = 1.3$ obtained from the ensemble FRET measurements (Fig. 2b), consistent with an approximate two-state folding behavior. The parameter $\beta = n^{\ddagger}/n$ provides a measure of the position of the transition state[25] and has been applied in protein folding[26,27]. For the Twister ribozyme, $\beta_F = 0.37$ and $\beta_U = 0.72$, suggesting that the transition state ensemble (TSE) for tertiary folding lies somewhat closer to the unfolded state than to the folded state[25] (Supplementary Fig. 10). The folding kinetics of the Twister ribozyme is remarkably similar to the docking and undocking rates of the two-way junction hairpin ribozyme at different $MgCl_2$ concentrations in 0.5 M NaCl[24], despite their very different tertiary structures. In both RNAs, Mg^{2+} ions only partially stabilize the TSE, which presumably is reached soon after the RNA helices begin to interact. A partially expanded TSE was observed for refolding of the much larger (398 nt) *Tetrahymena* ribozyme in Mg^{2+} and spermidine ($\beta_F \approx 0.15$)[28]. By contrast, for the hairpin ribozyme in low salt, and for many small proteins, the TSE lies closer to the native state[29].

Kinetics of Twister RNA folding

The Hidden Markov analysis of the steady-state FRET traces is useful for understanding the equilibrium dynamics of the folded RNA, but lacks information about the initial folding events. Therefore, we also measured the initial folding kinetics by injecting $MgCl_2$ into slide chambers during single-molecule experiments. We immobilized Twister RNA to the quartz slide in imaging buffer lacking Mg^{2+}, then flowed in imaging buffer containing 10 mM $MgCl_2$ (Fig. 4c) while continuously recording the Cy3 and Cy5 intensity. Free Cy3 fluorophores were included in the injected buffer to track the arrival of $MgCl_2$. A two-dimensional FRET histogram aligned to the moment of Mg^{2+} addition showed that the molecules start to move from the low-FRET state to the high-FRET state soon after they interact with Mg^{2+} ions (Fig. 4d). After 10 s, the molecules steadily fluctuated between

high-FRET and low-FRET states as observed in our equilibrium smFRET experiments. The average increase in the population of the high FRET state after the addition of $MgCl_2$ corresponded to $k_{obs} = 0.2\ s^{-1}$ (Supplementary Fig. 11), in good agreement with $k_{obs} = k_F + k_U = 0.15\ s^{-1}$ at 10 mM $MgCl_2$ calculated from the Hidden Markov analysis. This result indicates that the first folding event is similar to subsequent folding events.

Effects of divalent salts on folding and catalysis

We compared the catalytic activity and folding of the Twister ribozyme in the presence of different divalent chloride salts. Surprisingly, the midpoints for the extent of self-cleavage in the presence of $MnCl_2$ and $ZnCl_2$ were 56 μM and 51 μM, respectively, lower than the midpoint for self-cleavage in the presence of $MgCl_2$ (135 μM) (Fig. 5a). The greater effectiveness of Mn^{2+} and Zn^{2+} was likely due to better folding of the Twister ribozyme in the presence of transition metal ions, as the midpoints for ensemble folding were 1.7 mM Mn^{2+} and 1.4 mM Zn^{2+}, respectively, much lower than the midpoint for folding in Mg^{2+} (10 mM) (Fig. 5b). By contrast, cationic radius seemed unimportant, because the fraction of folded RNA increased similarly with the concentration of larger Ca^{2+} and Ba^{2+} ions as with Mg^{2+} ions (Fig. 5b and Supplementary Table 2).

We also compared the folding behavior of single Twister ribozymes at 2 mM $MgCl_2$, $MnCl_2$ or $ZnCl_2$ using single-molecule FRET (Fig. 5c). The frequency of transitions to the folded state was similar in the presence of each cation, but the lifetime of the folded state was shorter in Mg^{2+} than in Mn^{2+} or Zn^{2+} ions, resulting in a higher population of folded RNA in Mn^{2+} or Zn^{2+} (Fig. 5d). These data clearly suggest that at 2 mM concentration, Mn^{2+} or Zn^{2+} ions stabilize the folded state better than Mg^{2+} ions.

Finally, we asked how efficiently different metal ions activate Twister self-cleavage, including the transition metal ions Mn^{2+}, Fe^{2+}, Co^{2+}, Ni^{2+} and Zn^{2+}. In all cases, lower amounts of transition metal ions than alkaline earth metal ions were needed to support Twister activity. Ni^{2+} was most effective among the metal ions tested, with 12 μM $NiCl_2$ sufficient for half-maximal activity (Fig. 5e). In general, the concentration needed to reach half-maximal activity approximately correlated with the expected bond strength of the transition metal ions tested[30]. As discussed below, this unusual preference for transition metals suggests that the Twister ribozyme may respond to the presence of such ions in rice and other organisms.

DISCUSSION

Although Mg^{2+} ions stabilize the folded states of RNA, many ribozymes require high Mg^{2+} ion concentrations for their activity[3]. Metal ion binding within the RNA active site often requires an energetically unfavorable reorganization of the RNA conformation, partial dehydration of the metal ion, or both[31,32]. Mg^{2+} ions directly coordinate the scissile phosphodiester, orient bases for proton transfer while compensating for the accumulation of negative charge in the transition state for self-cleavage, or simply stabilize tertiary interactions within the active site, which are often weaker than those in the periphery of the folded RNA[33]. Remarkably, Twister was reported to show almost no selectivity for Mg^{2+} ions during self-cleavage[2], consistent with an absence of ordered active site metal ions in

several crystal structures[7,34], although there is evidence that a Mg^{2+} ion coordinates the non-bridging phosphate oxygens at the cleavage site in the *env22* Twister ribozyme[8].

Our results support the idea that metal ions mainly act by stabilizing the functional structure of the Twister ribozyme, because metal ions that activate the ribozyme at low metal ion concentrations also stabilize the folded RNA more efficiently than Mg^{2+}. For the metal ions for which we can directly compare folding and self-cleavage rates, the ribozyme activity increases proportionally less than the stability of the folded RNA, suggesting that transition metal ions interact with the folded ribozyme slightly differently than Mg^{2+} ions (Fig. 5). Achieving a compact, high FRET state is not sufficient for catalysis, as we are unable to detect cleaved products of the G47A-G48A mutant (Supplementary Fig. 9), although this RNA measurably populates the high FRET state (Fig. 3b). This is consistent with the idea that reorganization of the active site pocket is needed after both pseudoknots base pair[35].

It is remarkable that only transient folding is sufficient for *Osa* Twister catalysis, indicating that reorganization of the catalytic core must occur rapidly after the initial folding step. This is somewhat different from the heterogeneous folding kinetics of *env22* Twister.[13] Extrapolating our measured folding rates (Fig. 4b) to 50 μM $MgCl_2$, we obtain a time constant for folding τ_F = 170 s, only slightly shorter than the time constant for self-cleavage of the biomolecular form of the ribozyme (τ_{cleave} = 250 s). A similar logic applied to our self-cleavage and folding rates in 0.5 mM $MgCl_2$, assuming a five- to tenfold destabilization of the folded RNA by our FRET labels (τ_{cleave} = 7 s ≤ τ_F ≈ 17 s), suggests that every folding event results in self-cleavage, on average.

Although Mg^{2+} ions usually promote RNA folding and catalysis in the cell, the recent discoveries of riboswitches that recognize Ni^{2+}, Co^{2+} and Mn^{2+} demonstrate that transition metals can be selectively recognized by non-coding RNAs[36]. No natural ribozymes are known to preferentially use transition metals over Mg^{2+}, but the minimal hammerhead ribozyme self-cleaves in the presence of divalent ions such as Mn^{2+}, Co^{2+}, Sr^{2+} and Ba^{2+} (ref. 37), and the *in vitro* selected lead ribozyme self-cleaves in transition metals when supplemented with Mg^{2+} (ref. 38). Unlike these examples, *Osa* Twister folds and reacts in 10–100 μM transition metal ions, concentrations comparable to the binding constants of the Ni, Co and Mn riboswitches[4,5]. Our analysis of Twister self-cleavage does not account for oxidation of the metal ion or interactions with the Cl^- anion, and may underestimate the efficiency of transition metal ion activation.

These results raise the interesting question of whether transition metals specifically stabilize the active conformation of Twister ribozyme. Surveys of known nucleic acid structures confirm that transition metal ions preferentially coordinate the N7 of purines[39,40]. In the metal-sensing riboswitches, the Mn^{2+} or Co^{2+} ions bridge N7 atoms of conserved purines while coordinating nearby phosphodiesters, usually through hydrogen bonds with metal-bound water molecules. These metal ion interactions pinch together helices in different parts of the riboswitch, and serve as part of the switch mechanism. In crystallographic structures of *Osa* and *env22* Twister ribozymes, hydrated Mg^{2+} ions occupy a pocket adjacent to the scissile phosphodiester, the major groove of pseudoknot 2, and the linker between P4 and pseudoknot 1[7,8]. In the *Osa* ribozyme, these grooves are lined with G N7 atoms that face

inward toward phosphate groups on either side of the cleavage site (Fig. 5d), offering a plausible explanation for strong transition metal binding to the *Osa* Twister RNA.

The function of the Twister ribozyme in the host organism *O. sativa* is not known. Rice seedlings rapidly take up Mg^{2+} from the root tips, and Mg^{2+} deficiency causes leaf yellowing and other growth defects[41]. Rice also concentrates certain transition metals in its tissue, some of which are essential micronutrients[42,43]. Our results show that transient folding in micromolar metal ion is sufficient for robust activity. Its preference for transition metal ions and small size make Twister a potentially attractive starting point for engineered ribozymes that respond to rare or toxic metals in rice and other organisms.

METHODS

Methods and any associated references are available in the online version of the paper.

ONLINE METHODS

RNA preparation

The Twister ribozyme variants used in this study were based on 54 nt long *Osa 1-4* sequence from *O. sativa*[7]. Activity assays were performed using a two-stranded form of the ribozyme with an extended P3 helix as previously described[2]. The substrate RNA containing the cleavage site, Ost-S: 5′ rCCGCCUAACUCCGCCUAUGUCAU 3′ was purchased from IDT, USA and purified by 20% PAGE. The ribozyme strand Ost-Ri: 5′ rGGAUGAUAUAGCCGGUCCCAAGCCCGGAAAAGGAGGAGGGGGCGG 3′ was transcribed *in vitro* using a double-stranded template DNA (Invitrogen) and gel purified before use.

For fluorescence folding experiments, a unimolecular variant of *Osa* Twister with a short P3 helix was prepared by splint ligation of two fragments with T4 RNA ligase I as described in Solomatin and Herschlag[44]. Synthetic RNA fragments were purchased from IDT in a reverse phase HPLC purified form. The 5′ fragment, 5′ rCCGCCdUrAACACUGCCAAUGCCGG-(Cy3)-UCCCA 3′, contains Cy3 inserted in the backbone of the RNA between G14 and U15 (Int Cy3; IDT). To prevent phosphodiester bond cleavage, U6 was replaced with dU. The 3′ fragment was extended with deoxyribonucleotides to hybridize with an Cy5-labeled anchor DNA: 5′ r(AGCCCGGAUAAAAGUGGAGGGGGCGG) d(AGGACGACACACTTTGGACAGGACACACAGGACACAGG) 3′. The ligated product (OstS5-Cy3) was separated from the reactants by 20% PAGE and then extensively exchanged with 1X HK buffer (30 mM K-HEPES, pH 7.5; 100 mM KCl). Anchor DNA oligomers were purchased from IDT: (SA5-Cy5: 5′ dCCTGTGTCCTGTGTGTCCTGTCCAAAGTGTGTCGTCC-(Cy5) 3′; SA5-BHQ2: 5′dCCTGTGTCCTGTGTGTCCTGTCCAAAGTGTGTCGTCC-(BHQ2) 3′ and Bio-SA5-Cy5: 5′ (Biotin)-dCCTGTGTCCTGTGTGTCCTGTCCAAAGTGTGTCGTCC-(Cy5) 3′.

Ribozyme activity assays

Self-cleavage assays for the bimolecular form of the ribozyme were performed as previously described[2]. 5 nM 5′-[^{32}P] labeled substrate strand (Ost-S) and 100 nM ribozyme strand

(Ost-Ri) in 1 X HK buffer (8 μL) were heated to 75 °C for 5 min and slowly cooled to room temperature (20 °C). To start the reaction, 2 μl divalent salts from 5X stocks in deionized water of different concentrations were added and incubated at room temperature for a specific time period mentioned in the figure legends of individual experiments. An equal volume of stop solution (90% formamide, 50 mM EDTA, 0.05% xylene cyanol and 0.05% bromophenol blue) was added to terminate the reaction. The products were separated from the substrate RNA by denaturing 16% PAGE and quantified using a Storm phosphorimager (GE Healthcare). All the divalent metal chloride salts were purchased from Sigma-Aldrich (USA). Stock solutions of the salts were made in deionized (18 MOhm) water and filtered through a 0.22 μm membrane before storing at 4 °C. Solutions of transition metal salts, especially $FeCl_2$, $CoCl_2$, $NiCl_2$ and $CdCl_2$, were prepared with degassed water and used immediately.

For the activity assay using the chemically synthesized (IDT) unimolecular form of the ribozyme, 1 μM unlabeled full length *Osa*-Twister RNA in 1X HK buffer (8 μL) were heated to 75 °C for 5 min and cooled to room temperature (20 °C). The reactions were started with 2 μl $MgCl_2$ from 5X stocks and stopped after 1 min at room temperature as described before. The products were separated from the full length RNA by denaturing 16% PAGE, stained with SYTO RNASelect (ThermoFisher) and quantified using a Typhoon 9410 scanner (GE Healthcare).

For co-transcriptional self cleaving assays, T7 transcription reactions were carried out *in vitro* with WT or mutated DNA templates for the *Osa 1-4* Twister ribozyme for 30 min at 37 °C. 40 μL transcription reactions contained 4 μL 10X T7 transcription buffer, 4 μL 10X low ATP NTPs (1.25 mM ATP, 5 mM CTP, 5 mM GTP and 5 mM UTP), 0.5 μg DNA template, 20 μCi α-[^{32}P] ATP, 1 μL T7 polymerase. The transcribed RNAs were passed through TE30 Chroma spin columns (Clontech, USA), and the full length RNA (54 nt) and 3′ product (3′P: 48 nt) were separated using 16% PAGE.

RNase T1 footprinting

A mixture of 100 nM 5′-[^{32}P]-labeled *Osa*-Twister dU6 RNA (single chain) and 1 μM unlabeled *Osa*-Twister dU6 RNA in 8 μL 1X HK buffer were incubated at 75 °C for 5 min, followed by 37 °C for 15 min and room temperature for 5 min. 2 μL $MgCl_2$ solutions from 5X stocks were added to the mixture and incubated an additional 5 min at room temperature. RNase T1 was added at a final concentration of 0.02 U/μl and incubated 5 min at room temperature. Reactions were quenched with an equal volume of formamide loading dye and immediately loaded on a 16% sequencing gel.

Ensemble FRET

To measure the extent of folding by FRET, 20 nM OstS5-Cy3 was annealed with 40 nM SA5-Cy5 DNA in 400 μl of 1 X HK buffer by incubating the mixture at 75 °C for 5 min, 37 °C for 15 min and finally equilibrated at 30 °C for 5 min. The fluorescence emission of Cy3 and Cy5 were measured in a Fluorolog 3 (Horiba) spectrofluorometer by exciting the samples at 540 nm and measuring the emissions at 565 nm and 663 nm respectively. Ribozyme samples were titrated with salt stock solutions and incubated for 2 min at 30 °C

between measurements. FRET efficiencies were calculated from $E_{FRET} = I_{663}/(I_{565} + I_{663})$. Fractional folding, f_F, at different divalent salt concentrations was fit to the Hill equation,

$$f_F = (E_i - E_0)/(E_\alpha - E_0) = [M^{2+}]^n/(K^n + [M^{2+}]^n)$$

in which E_0 is the FRET efficiency in 1X HK, E_α is the maximum FRET efficiency in saturating salt, $[M^{2+}]$ is the divalent salt concentration, K is the folding midpoint and n is the Hill coefficient, which is a measure of the gradient of the equilibrium $\partial \ln K/\partial \ln[M^{2+}]$.

Single-molecule FRET measurements

For single-molecule experiments, 20 nM OstS5-Cy3 and 40 nM Bio-SA5-Cy5 DNA in 10 μL 1X HK were annealed as described above and equilibrated at RT for 5 min. Samples were diluted 400 times in the imaging buffer (IB: 30 mM HEPES, pH 7.5; 100 mM KCl; 0.8% glucose and 4 mM Trolox) and immobilized on quartz slides coated with DDS and pre-treated with biotinylated BSA, Tween 20 and Neutravidin[45]. Imaging buffer containing the specified concentration of divalent salt, 0.1 mg/ml glucose oxidase (Sigma) and 0.02 mg/ml catalase (Sigma) were flowed in to the slide chambers before imaging. smFRET traces were recorded using a home-built TIRF microscope with an EMCCD camera (Andor), as described previously[20,46]. The time resolution of each movie was 0.1 s / frame if not stated otherwise, and ten frames of Cy5 excitation were used at the beginning and end of each recorded movie to verify the presence of FRET acceptors in each molecule selected for analysis.

Single-molecule data analysis

Molecules were picked and trajectories for individual molecules were extracted from movies using a custom IDL code as described previously[45]. Only trajectories containing both the FRET donor and acceptor were selected for further analysis. We calculated the FRET efficiency with leakage correction: $E_{FRET} = (I_A - L_f * I_D)/[I_D + (I_A - L_f * I_D)]$, in which I_D and I_A are the fluorescence intensities of the donor (Cy3) and the acceptor (Cy5) respectively and L_f is the leakage factor for the TIRF microscope. Histograms of FRET efficiency at different divalent salt concentrations were built using more than 200 molecules apiece. Individual trajectories were weighted so that each molecule contributed equally to the histogram regardless of the length of its trajectory before photobleaching. To build the histogram, 1) we built a histogram for each individual trajectory, with each frame of that trajectory as one data point; 2) we normalized each individual histogram so that each has a total area of 1; 3) we added all individual histograms together to get an overall histogram; 4) we divided the overall histogram by a factor equal to the total number of trajectories used and the frequencies were labeled as “relative counts” in the y- axes. FRET histograms were fitted to a double Gaussian using Origin (OriginLab), and the absolute fractional folding calculated from $A_{hF}/(A_{lF}+A_{hF})$, where A_{lF} and A_{hF} are the areas under the low FRET and high FRET peaks, respectively. HaMMy was used to calculate the transition rates between folded and unfolded states[47]. All custom software and codes mentioned above are available upon request. For flow-in experiments, 5 nM Cy3 was co-injected with the imaging buffer containing 10 mM $MgCl_2$ while recording continuously with a time resolution of 30 ms. 100

selected trajectories were aligned based on the time when $MgCl_2$ reached the molecule, as determined by a small rise in the Cy3 background. The 2D histogram was generated using Origin.

Supplementary Material

Refer to Web version on PubMed Central for supplementary material.

Acknowledgments

The authors thank K. Sarkar and S. Abeysirigunawardena for their assistance and M. Greenberg, K. Karlin and J. Morrow for helpful discussion.

This work was supported by a grant from the NSF [MCB-1616081 to S.W.] and the NIH [GM 065367 to T.H.].

References

1. Jimenez RM, Polanco JA, Luptak A. Chemistry and Biology of Self-Cleaving Ribozymes. Trends Biochem Sci. 2015; 40:648–661. [PubMed: 26481500]
2. Roth A, et al. A widespread self-cleaving ribozyme class is revealed by bioinformatics. Nat Chem Biol. 2014; 10:56–60. [PubMed: 24240507]
3. Weinberg Z, et al. New classes of self-cleaving ribozymes revealed by comparative genomics analysis. Nat Chem Biol. 2015; 11:606–610. [PubMed: 26167874]
4. Furukawa K, et al. Bacterial riboswitches cooperatively bind Ni(2+) or Co(2+) ions and control expression of heavy metal transporters. Mol Cell. 2015; 57:1088–1098. [PubMed: 25794617]
5. Price IR, Gaballa A, Ding F, Helmann JD, Ke A. Mn(2+)-sensing mechanisms of yybP-ykoY orphan riboswitches. Mol Cell. 2015; 57:1110–1123. [PubMed: 25794619]
6. DeRose VJ. Metal ion binding to catalytic RNA molecules. Curr Opin Struct Biol. 2003; 13:317–324. [PubMed: 12831882]
7. Liu Y, Wilson TJ, McPhee SA, Lilley DM. Crystal structure and mechanistic investigation of the twister ribozyme. Nat Chem Biol. 2014; 10:739–744. [PubMed: 25038788]
8. Ren A, et al. In-line alignment and Mg(2)(+) coordination at the cleavage site of the env22 twister ribozyme. Nat Commun. 2014; 5:5534. [PubMed: 25410397]
9. Wilson TJ, Liu Y, Domnick C, Kath-Schorr S, Lilley DM. The Novel Chemical Mechanism of the Twister Ribozyme. J Am Chem Soc. 2016; 138:6151–6162. [PubMed: 27153229]
10. Gaines CS, York DM. Ribozyme Catalysis with a Twist: Active State of the Twister Ribozyme in Solution Predicted from Molecular Simulation. J Am Chem Soc. 2016; 138:3058–3065. [PubMed: 26859432]
11. Zhang S, et al. Role of the active site guanine in the glmS ribozyme self-cleavage mechanism: quantum mechanical/molecular mechanical free energy simulations. J Am Chem Soc. 2015; 137:784–798. [PubMed: 25526516]
12. Gebetsberger J, Micura R. Unwinding the twister ribozyme: from structure to mechanism. Wiley Interdiscip Rev RNA. 2017; 8
13. Vusurovic N, Altman RB, Terry DS, Micura R, Blanchard SC. Pseudoknot Formation Seeds the Twister Ribozyme Cleavage Reaction Coordinate. J Am Chem Soc. 2017; 139:8186–8193. [PubMed: 28598157]
14. Kosutic M, et al. A Mini-Twister Variant and Impact of Residues/Cations on the Phosphodiester Cleavage of this Ribozyme Class. Angew Chem Int Ed Engl. 2015; 54:15128–15133. [PubMed: 26473980]
15. Ucisik MN, Bevilacqua PC, Hammes-Schiffer S. Molecular Dynamics Study of Twister Ribozyme: Role of Mg(2+) Ions and the Hydrogen-Bonding Network in the Active Site. Biochemistry. 2016; 55:3834–3846. [PubMed: 27295275]

16. Alatossava T, Jutte H, Kuhn A, Kellenberger E. Manipulation of intracellular magnesium content in polymyxin B nonapeptide-sensitized Escherichia coli by ionophore A23187. J Bacteriol. 1985; 162:413–419. [PubMed: 2984182]
17. Froschauer EM, Kolisek M, Dieterich F, Schweigel M, Schweyen RJ. Fluorescence measurements of free [Mg2+] by use of mag-fura 2 in Salmonella enterica. FEMS Microbiol Lett. 2004; 237:49–55. [PubMed: 15268937]
18. Zhong W, Schobert C, Komor E. Transport of magnesium ions in the phloem of Ricinus communis L. seedlings. Planta. 1993; 190:114–119.
19. Ha T, et al. Probing the interaction between two single molecules: fluorescence resonance energy transfer between a single donor and a single acceptor. Proc Natl Acad Sci U S A. 1996; 93:6264–6268. [PubMed: 8692803]
20. Roy R, Hohng S, Ha T. A practical guide to single-molecule FRET. Nat Methods. 2008; 5:507–516. [PubMed: 18511918]
21. Kilburn D, Roh JH, Guo L, Briber RM, Woodson SA. Molecular crowding stabilizes folded RNA structure by the excluded volume effect. J Am Chem Soc. 2010; 132:8690–8696. [PubMed: 20521820]
22. Paudel BP, Rueda D. Molecular crowding accelerates ribozyme docking and catalysis. J Am Chem Soc. 2014; 136:16700–16703. [PubMed: 25399908]
23. Dupuis NF, Holmstrom ED, Nesbitt DJ. Molecular-crowding effects on single-molecule RNA folding/unfolding thermodynamics and kinetics. Proc Natl Acad Sci U S A. 2014; 111:8464–8469. [PubMed: 24850865]
24. Bokinsky G, et al. Single-molecule transition-state analysis of RNA folding. Proc Natl Acad Sci U S A. 2003; 100:9302–9307. [PubMed: 12869691]
25. Leffler JE. Parameters for the Description of Transition States. Science. 1953; 117:340–341. [PubMed: 17741025]
26. Tanford C. Protein denaturation. C. Theoretical models for the mechanism of denaturation. Adv Protein Chem. 1970; 24:1–95. [PubMed: 4912353]
27. Jackson SE, Fersht AR. Folding of chymotrypsin inhibitor 2. 1. Evidence for a two-state transition. Biochemistry. 1991; 30:10428–10435. [PubMed: 1931967]
28. Koculi E, Thirumalai D, Woodson SA. Counterion charge density determines the position and plasticity of RNA folding transition states. J Mol Biol. 2006; 359:446–454. [PubMed: 16626736]
29. Sosnick TR. Kinetic barriers and the role of topology in protein and RNA folding. Protein Sci. 2008; 17:1308–1318. [PubMed: 18502978]
30. Irving H, Willams RJP. Order of Stability of Metal Complexes. Nature. 1948; 162:746–747.
31. Woodson SA. Metal ions and RNA folding: a highly charged topic with a dynamic future. Curr Opin Chem Biol. 2005; 9:104–109. [PubMed: 15811793]
32. Draper DE, Grilley D, Soto AM. Ions and RNA folding. Annu Rev Biophys Biomol Struct. 2005; 34:221–243. [PubMed: 15869389]
33. Ward WL, Plakos K, DeRose VJ. Nucleic acid catalysis: metals, nucleobases, and other cofactors. Chem Rev. 2014; 114:4318–4342. [PubMed: 24730975]
34. Eiler D, Wang J, Steitz TA. Structural basis for the fast self-cleavage reaction catalyzed by the twister ribozyme. Proc Natl Acad Sci U S A. 2014; 111:13028–13033. [PubMed: 25157168]
35. Kobori S, Yokobayashi Y. High-Throughput Mutational Analysis of a Twister Ribozyme. Angew Chem Int Ed Engl. 2016; 55:10354–10357. [PubMed: 27461281]
36. Saunders AM, DeRose VJ. Beyond Mg2+: functional interactions between RNA and transition metals. Curr Opin Chem Biol. 2016; 34:152–158. [PubMed: 27616014]
37. Dahm SC, Uhlenbeck OC. Role of divalent metal ions in the hammerhead RNA cleavage reaction. Biochemistry. 1991; 30:9464–9469. [PubMed: 1716459]
38. Pan T, Uhlenbeck OC. A small metalloribozyme with a two-step mechanism. Nature. 1992; 358:560–563. [PubMed: 1501711]
39. Leonarski F, D'Ascenzo L, Auffinger P. Binding of metals to purine N7 nitrogen atoms and implicationsfor nucleic acids: A CSD survey. Inorg Chim Acta. 2016; 452:82–89.

40. Sigel RK, Sigel H. A stability concept for metal ion coordination to single-stranded nucleic acids and affinities of individual sites. Acc Chem Res. 2010; 43:974–984. [PubMed: 20235593]

41. Kobayashi NI, Tanoi K. Critical Issues in the Study of Magnesium Transport Systems and Magnesium Deficiency Symptoms in Plants. Int J Mol Sci. 2015; 16:23076–23093. [PubMed: 26404266]

42. Yoneyama T, Ishikawa S, Fujimaki S. Route and Regulation of Zinc, Cadmium, and Iron Transport in Rice Plants (Oryza sativa L.) during Vegetative Growth and Grain Filling: Metal Transporters, Metal Speciation, Grain Cd Reduction and Zn and Fe Biofortification. Int J Mol Sci. 2015; 16:19111–19129. [PubMed: 26287170]

43. Takahashi R, Bashir K, Ishimaru Y, Nishizawa NK, Nakanishi H. The role of heavy-metal ATPases, HMAs, in zinc and cadmium transport in rice. Plant Signal Behav. 2012; 7:1605–1607. [PubMed: 23072989]

44. Solomatin S, Herschlag D. Methods of site-specific labeling of RNA with fluorescent dyes. Methods Enzymol. 2009; 469:47–68. [PubMed: 20946784]

45. Hua B, et al. An improved surface passivation method for single-molecule studies. Nat Methods. 2014; 11:1233–1236. [PubMed: 25306544]

46. Kim H, et al. Protein-guided RNA dynamics during early ribosome assembly. Nature. 2014; 506:334–338. [PubMed: 24522531]

47. McKinney SA, Joo C, Ha T. Analysis of single-molecule FRET trajectories using hidden Markov modeling. Biophys J. 2006; 91:1941–1951. [PubMed: 16766620]

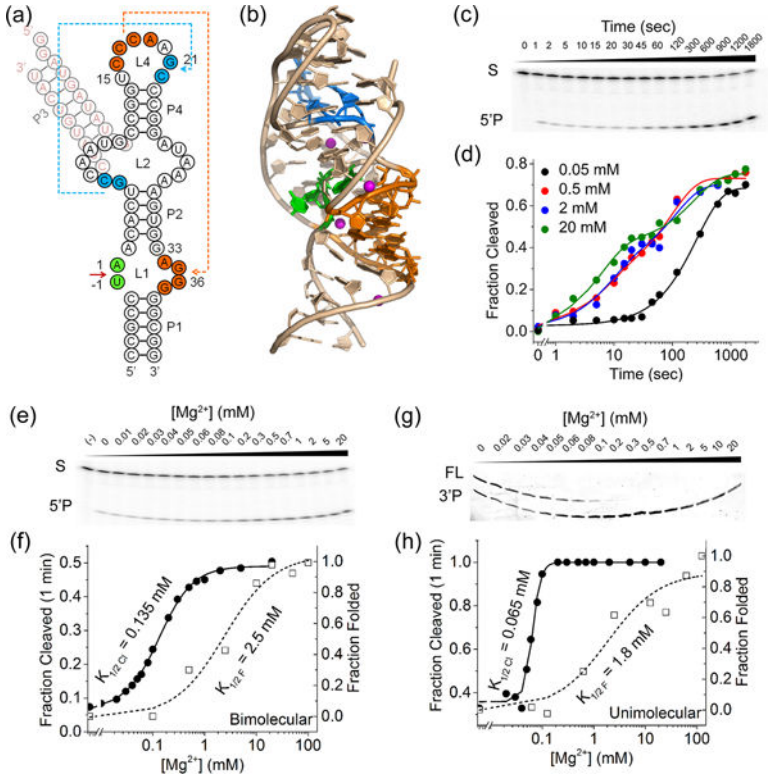

Fig 1. Self-cleavage of a minimal *Oryza sativa* Twister ribozyme at low Mg^{2+}

(**a**) Secondary structure of *Osa 1-4* Twister ribozyme[2]. Pseudoknots 1 and 2 are blue and orange, respectively. The arrowhead represents the cleavage site. A P3 stem (faded red letters) was added to *Osa 1-4* to stabilize base pairing between substrate (S) and ribozyme (R) strands of bi-molecular ribozymes for activity assays. (**b**) Structure of *Osa 1-4* Twister ribozyme (pdb: 4OJI[7]) colored as in **a**. Mg^{2+} ions are shown as magenta spheres. (**c**) Representative 16% PAGE image showing the consumption of substrate (S) and appearance of product (5′P) with time. (**d**) Progress curves were fitted to single or double exponential rate equations: $f_{cleaved} = I_{5'P}/(I_S+I_{5'P}) = A_{fast}[1–\exp(-k_{fast}t)] + A_{slow}[1–\exp(-k_{slow}t]$. The rate constants are listed in Supplementary Table 1 (n = 3; s.d. <10%). (**e**) Cleavage reactions of the bimolecular riboyzme in different $MgCl_2$ concentrations were stopped after 1 min and analyzed by denaturing 16% PAGE. (**f**) The fraction cleaved after 1 min versus Mg^{2+} concentration (filled symbols) was fit to the Hill equation (solid line). n = 3; s.d. < 10%. Relative folding of the bimolecular ribozyme by RNase T1 protection of G21 with $MgCl_2$ concentration (open symbols; Supplementary Fig. 3) was fit to the Hill equation (dashed line) with a midpoint of 2.5 mM $MgCl_2$. (**g**) Self-cleavage of the unimolecular ribozyme after 1 min in different $MgCl_2$ concentrations, as in **d**. (**h**) The fraction cleaved (filled symbols and solid line) and RNase T1 protection (open symbols and dashed line; see Supplementary Fig. 2) were fit to the Hill equation as in **f**; n = 3.

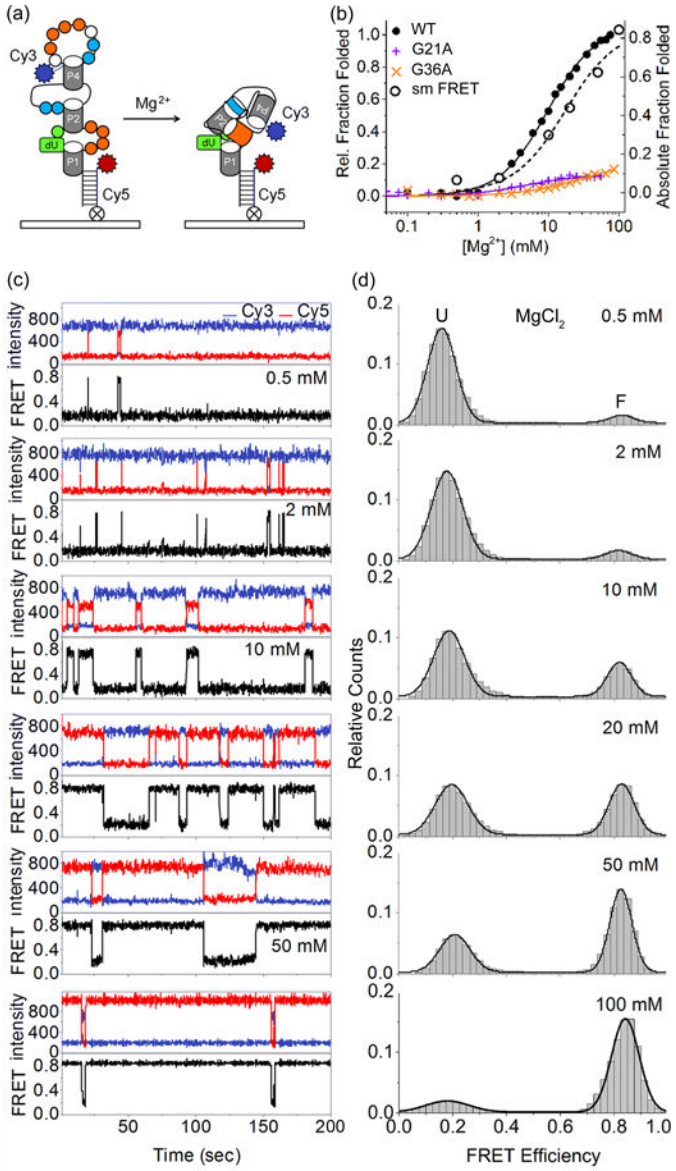

Fig 2. Folding of Twister ribozyme in $MgCl_2$

(**a**) The FRET assay for folding. Cy5 is attached to a DNA strand hybridized to a 3′ extension of the ribozyme; Cy3 is attached to the phosphodiester backbone between G23 and U24. In the unfolded state, Cy3 and Cy5 dyes are far apart, resulting in low FRET (left). In the presence of Mg^{2+}, pseudoknot formation brings Cy3 and Cy5 together, resulting in high FRET (right). Self-cleavage is prevented by a deoxyribose at the cleavage site. (**b**) Relative fraction of folded RNA (See Supplementary Table 2 for parameters and error analysis) as a function of $MgCl_2$ concentration, from ensemble FRET at 30 ˚C (filled symbols; left axis) or smFRET at 20 ˚C (open symbols; right axis). (**c**) smFRET traces at different $MgCl_2$ concentrations show fluctuations between the low-FRET unfolded state and high-FRET folded state. Blue, Cy3 intensity; red, Cy5 intensity; black, FRET efficiency. With increasing $MgCl_2$, each molecule spends a longer time in the high FRET state. (**d**) FRET histograms of Twister ribozyme at various $MgCl_2$ concentrations showing that total

occupancy of the high-FRET state increases with $MgCl_2$. The histograms were fit to a double Gaussian (black line).

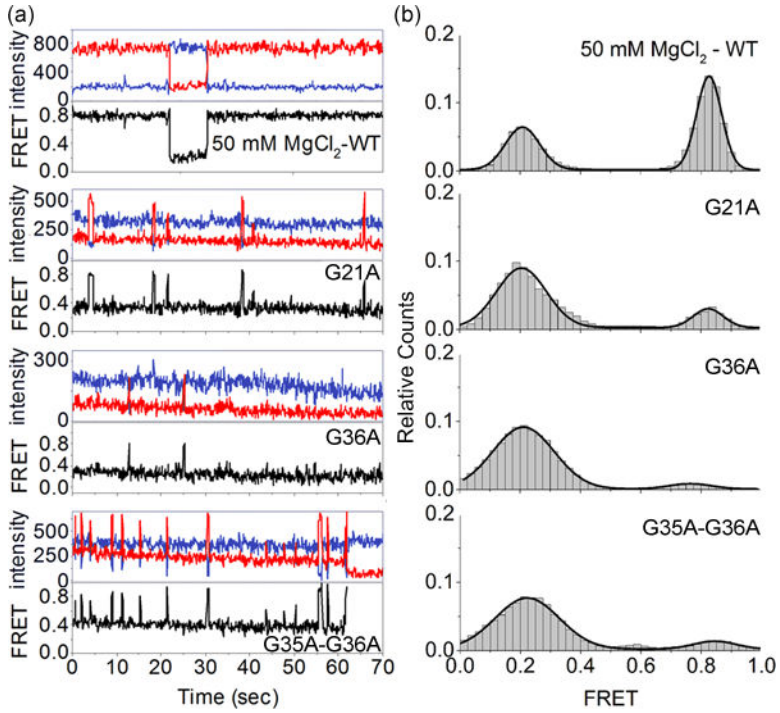

Fig 3. Pseudoknot mutations impair folding

(**a**) smFRET traces of WT, G21A, G36A and G35A-G36A Twister ribozymes at 50 mM $MgCl_2$. Twister mutants visited the high FRET folded state infrequently. (**b**) FRET histograms as in Figure 2d.

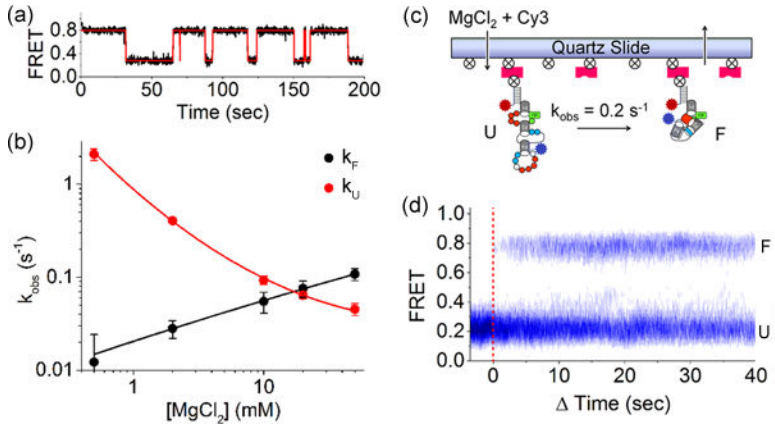

Fig 4. Kinetics of RNA folding

(**a**) A representative experimental FRET trace (black) with idealized FRET trace (red) generated by the HaMMy algorithm. (**b**) Relaxation rate constants for folding (black) and unfolding (red) versus Mg^{2+} ion concentration at room temperature. The rate constants were fit to a binding model with Mg^{2+} midpoints of saturation 21 (±9) mM and <1 (±0.1) mM for k_F and k_U, respectively. (**c**) Schematic of the single-molecule folding kinetics experiment. Imaging buffer plus 10 mM $MgCl_2$ and 5 nM Cy3 dye was added to the slide chamber containing immobilized Cy3-Twister•Cy5-SA5 complexes while recording continuously. The increase in background from free Cy3 marked the diffusion of Mg^{2+}-containing buffer. (**d**) Probability density maps of synchronized Twister FRET dynamics. The red dotted line indicates the moment Mg^{2+} ions interacted with the Twister complex. Before the addition of Mg^{2+}, all the molecules were in the 0.2 FRET state. After interacting with Mg^{2+}, molecules start fluctuating between the 0.2 and 0.8 FRET states before reaching equilibrium after 5 s.

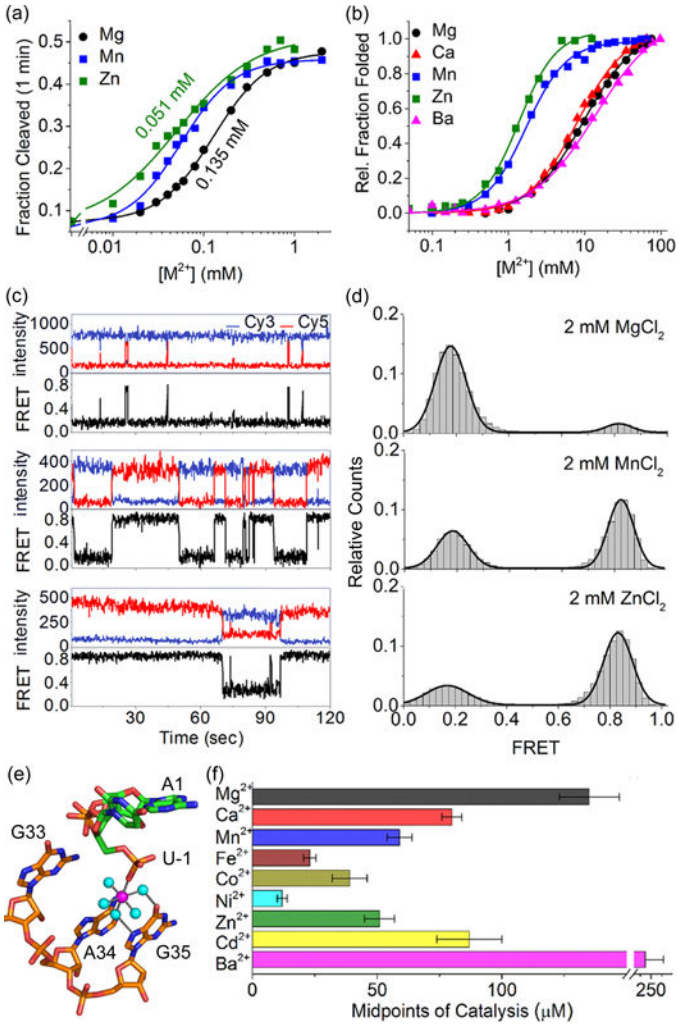

Fig 5. Twister is efficiently activated by transition metal ions

(**a**) Twister ribozyme activity after 1 min in $MgCl_2$, $MnCl_2$, and $ZnCl_2$ as in Figure 1d. The midpoints of catalysis for $MgCl_2$, $MnCl_2$, and $ZnCl_2$ were 135 (± 12) μM, 59 (± 5) μM and 51 (± 6) μM, respectively. Values are the mean and s.d. of 2–4 independent trials. (**b**) Folding in the presence of the divalent ions shown in the key by ensemble FRET at 30 ˚C. The fraction folded was fit to a two-state model as shown in Figure 2b. The folding midpoints were 10 (± 1) mM $MgCl_2$, 1.7 (± 0.4) mM $MnCl_2$ and 1.4 (± 0.3) mM $ZnCl_2$ (± s.d.; n = 2). (**c**) smFRET traces and (**d**) FRET histograms at 2 mM $MgCl_2$, 2 mM $MnCl_2$ and 2 mM $ZnCl_2$. Colors are as in Figure 2c. The high-FRET population follows the trend Mg^{2+} < Mn^{2+} < Zn^{2+}, suggesting that Twister folds more efficiently in the presence of transition metal ions. (**e**) Co-ordination of a hydrated Mg^{2+} ion between U-1, A34 and G35. Transition metal ions are expected to directly coordinate G N7 and interact with the phosphodiester indirectly through a water molecule. (**f**) Midpoints of self-cleavage in the presence of different divalent salts were determined as described in **a** and summarized as a horizontal bar graph. Error bars are s.d. of 2–3 independent trials.